DOI 10.5162/Ultrasonic2025/E5-b3

Reflection and Attenuation Analysis of Ultrasonic Pitch-Catch Measurement in Oil Wells with Casing Irregularity

Feng Cheng[1], *Xuelian Chen*[1*], *Jinlin Pan*[1], *Xihao Gu*[1], *Yali Zhou*[1], *and Xiaoming Tang*[1]
[1]*China University of Petroleum (East China), School of Geosciences, Qingdao, China*
B24010036@s.upc.edu.cn

Abstract: In cement-bonding evaluation, ultrasonic Lamb waves have been widely studied and applied in regular casing wells. However, its feasibility in irregular casing wells remains unknown. The relationship between ultrasonic Lamb waves and casing irregularity based on finite element time-domain simulation was investigated. According to the Lamb wave propagation, irregularity interfaces were determined by the Lamb wave attenuation and reflection wave amplitude changes. We propose a novel measurement method to detect surface unevenness of housings. This study assists in irregular casing cement-bonding evaluation.

Keywords: cementing quality evaluation, leaky lamb wave, attenuation, reflection

Introduction

The quality of cement bonding is crucial to ensure zonal isolation and well integrity. Traditional sonic logging assesses the quality of cement bonding using the amplitude of the casing wave throughout the life cycle of hydrocarbon wells. In recent years, the evaluation of ultrasonic cement has advanced significantly.

Zeroug and Froelich (2003) proposed integrating ultrasonic pulse-echo and pitch-catch measurements to distinguish gas, liquid, and cement behind the casing[1]. Viggen et al. (2016) employed the finite element method to simulate ultrasonic pitch-catch measurements, investigating the attenuation characteristics of through-tubing logging[2]. Brill and Klieber (2016) demonstrated that ultrasonic Lamb waves scatter and undergo mode conversion at discontinuous interfaces of layered structures[3]. Song et al. (2019) examined the effects of partial cement loss on ultrasonic pitch-catch logging[4]. This study investigates the scattering and mode conversion of ultrasonic Lamb waves at irregular interfaces in the casing caused by corrosion or perforation, focusing on variations in the amplitude, phase, and attenuation of the received waves. Based on the analysis results, a novel measurement and analysis method is proposed to detect casing nonuniformity.

Theory and Methods of Lamb Wave Simulation

The Lamb wave modes propagating in the casing are divided into two types. For the symmetric mode, the in-plane displacement(u) is symmetric as Eq. (1) , while the out-of-plane displacement(w) is antisymmetric as Eq. (2).The antisymmetric mode exhibits the opposite behavior.

Symmetric modes

$$u = u_1 = \mathrm{i}kA_2 \cos(px_3) + qB_1 \cos(qx_3) \quad (1)$$

$$w = u_3 = -pA_2 \sin(px_3) - \mathrm{i}kB_1 \sin(qx_3) \quad (2)$$

Antisymmetric modes

$$u = u_1 = \mathrm{i}kA_1 \sin(px_3) - qB_2 \sin(qx_3) \quad (3)$$

$$w = u_3 = pA_1 \cos(px_3) - \mathrm{i}kB_2 \cos(qx_3) \quad (4)$$

Selective excitation of specific Lamb wave modes can be achieved through controlled boundary conditions based on the constitutive relationship of displacement fields. To investigate the scattering and mode conversion of Lamb waves at irregular interfaces, specific mode Lamb wave excitation is preferable. Mode conversion is directly confirmed when a distinct mode emerges at irregular interfaces. It is difficult for the oblique incidence method to excite specific mode Lamb waves, making it unclear whether other modes resulted from the discontinuity.

We apply antisymmetric and symmetric out-of-plane displacement boundary conditions on the outer side of the casing to generate pure symmetric and antisymmetric Lamb waves, respectively. The simulation results are illustrated in Fig. 1, with highly magnified images showing the distribution of the displacement vector field and its impact on the shape of the casing. The arrows in the figure indicate the vector representation of the particle displacement. The symmetric mode should not be considered merely as a type of in-plane vibration. As one moves along the mode, the ratio of in-plane to out-of-plane displacement changes. Particularly noteworthy are the changes observed on the outer surface of the structure. In the

DOI 10.5162/Ultrasonic2025/E5-b3

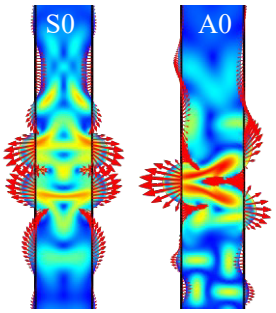

Fig. 1: S0 and A0 mode Lamb wave displacement field snapshot.

same way, antisymmetric modes cannot be considered as modes with only out-of-plane displacement values. The displacement associated with the S0 mode exhibits symmetry on both sides of the casing and appears as a compression wave. In contrast, the displacement corresponding to the A0 mode is identical on both sides of the casing and is characterized by a flexural waveform.

Fig. 2 shows the wave structures of the two modes along the thickness of the casing. For the symmetric mode, the in-plane displacement (u)is axially symmetric about the center of the casing thickness, while the out-of-plane displacement(w)is centrally symmetric about the center of the casing thickness(see 2a). For the antisymmetric mode, the in-plane displacement(u)is centrally symmetric about the center of the casing thickness, and the out-of-plane displacement(w)is axially symmetric about the center of the casing thickness(see 2b).

Leaky Lamb Wave Simulation in Irregular Casing

To simulate the effects of corrosion, the thickness of the upper casing was adjusted. Using the simulation method described above, S0-mode Lamb waves were excited in the casing. Fig. 3 illustrates the snapshots of the acoustic pressure field captured in the simulation model. At 60 μs, the in-phase pressure field in the casing indicates the exclusive presence of the S0 mode. At 100 μs, after passing through the irregular interface, the downward reflected wave is generated. At 140 μs, the out-of-phase pressure field in the casing indicates A0 mode. The array receivers were placed symmetrically on both sides of the casing in the model. The labels on the inside of the casing are RA and RA', while those on the outside are designated as RB and RB'. The resulting waveforms are presented in Fig. 4. As depicted in 4a, the waveform received at the source distance of 31 cm has already

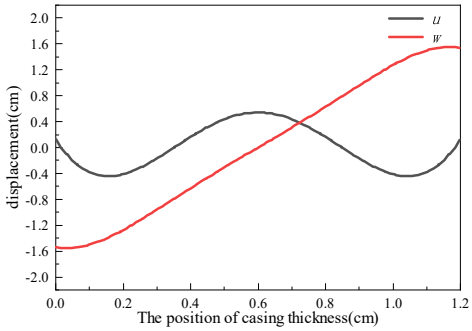

(a)

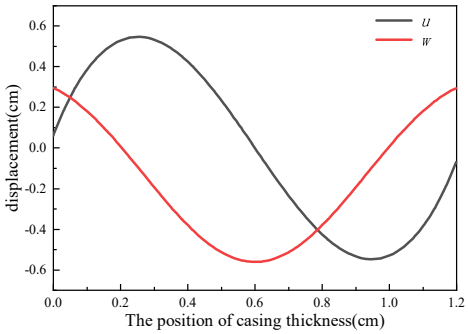

(b)

Fig. 2: Wave structure (a) S0 mode. (b)A0 mode.

been influenced by scattered waves. For the receiver at the source distance of 35 cm, the waveform displays an antisymmetric mode after 140 μs. In 4b, the reflected wave has been converted to the A0 mode. The results indicate that the irregular interface not only induces reflection and transmission phenomena but also causes mode conversion within the casing.

In pitch-catch logging, attenuation is calculated to assess the medium phase state behind the casing[5]. Irregular interfaces, such as those caused by casing corrosion, induce alterations in the waveforms of the two receivers. Moreover, reflections at these irregular interfaces cause significant attenuation. Attenuation increases with the degree of corrosion. Therefore, casing inhomogeneity leads to the scattering of Lamb waves. Placing receivers beyond the irregular results in a diminished amplitude and increased attenuation of the direct wave[6]. This increase in attenuation is independent of the medium behind the casing and the bonding condition. In addition to casing corrosion, perforation holes also generate irregular casing interfaces, which can also result in increased attenuation. Attenuation is maximized as the receivers span these perforations. Consequently, in pitch-catch logging results, perforation locations can be identified by analyzing local maxima in attenuation.

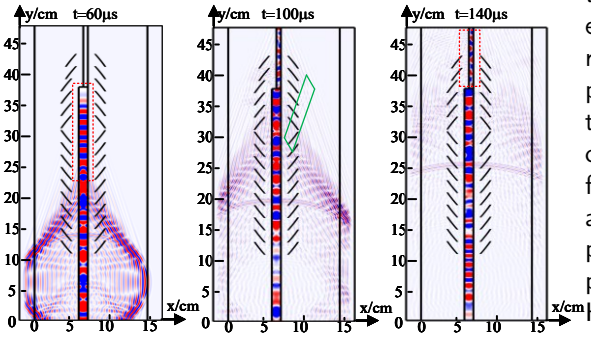

Fig. 3: Acoustic pressure field.

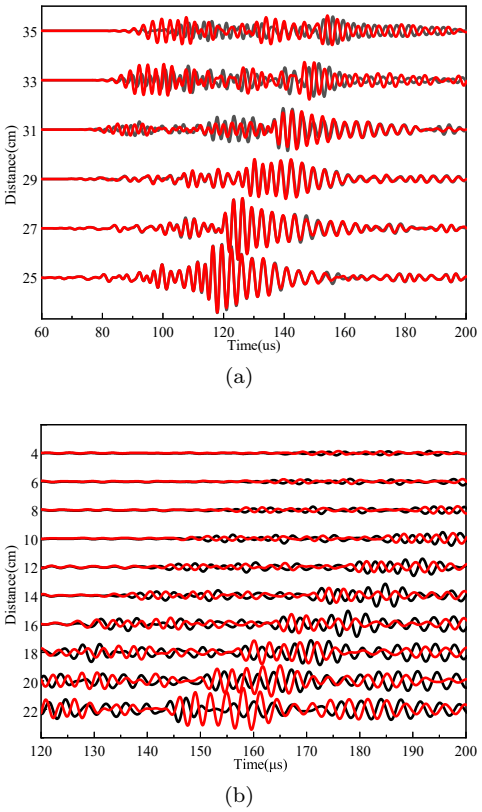

Fig. 4: (a)Transmission wave. (b) Reflection wave.

Application to Field Data

Fig. 5 compares the ultrasonic Lamb wave logging waveform and interpretation results for well X before and after perforation. The first trace represents depth (Depth). The second and third traces represent waveforms measured by the far receivers (Non-per F8; Per F8). The fourth and fifth traces represent the impedance behind the casing, both pre-and post-perforation (Non-per Im; Per Im). The sixth and seventh traces represent the attenuation calculated from the receiver waveforms (Non-per Att; Per Att). The eighth and ninth traces represent the medium states resulting from the ultrasonic pitch-catch logging data processing (Non-per SLG; Per SLG). Compared with the pre-perforation state, two significant changes were observed: firstly, the waveform amplitude in the perforation section was notably reduced; secondly, the attenuation result exhibited a "blocky" pattern after perforation. This "blocky" pattern indicated a good perforation condition from 1431.5 m to 1437.5 m. However, from 1437.5 m to 1441 m, the "blocky" pattern became less pronounced, indicating an ineffective perforation result.

Conclusion

In field production wells, inhomogeneous casing is common, leading to scattering and mode conversion at irregular interfaces during ultrasonic pitch-catch logging. The amplitude of the reflected wave serves as a reliable indicator for assessing the degree of non-uniformity in the casing. The transmitter can also function as a receiver, capturing reflected waves from irregular interfaces in the casing. Consequently, ultrasonic pitch-catch logging data from wells with non-uniform casings can be utilized to evaluate the degree of casing corrosion and estimate the non-leakage attenuation.

Acknowledgment

The authors express their gratitude to COSL for providing the field data used in this study. Furthermore, this work is supported by the National Natural Science Foundation of China (grant no. 42374156 and no. 41774141).

References

[1] S. Zeroug and B. Froelich. "Ultrasonic leaky-lamb wave imaging through a highly contrasting layer". In: *IEEE Symposium on Ultrasonics, 2003.* Vol. 1. 2003, 794–798 Vol.1. DOI: 10.1109/ULTSYM.2003.1293520.

[2] E. M. Viggen, T. F. Johansen, and I.-A. Merciu. "Simulation and modeling of ultrasonic pitch-catch through-tubing logging". In: *Geophysics* 81.4 (2016), pp. D383–D393.

[3] S. Zeroug et al. "Sonic and ultrasonic measurement applications for cased oil wells". In: *Insight-Non-Destructive Testing and Condition Monitoring* 58.8 (2016), pp. 423–430.

[4] R. Song, H. Dong, and X. Bao. "Numerical study of the effect of cement defects on flexural-wave logging". In: *Geophysics* 84.4 (2019), pp. D171–D177.

DOI 10.5162/Ultrasonic2025/E5-b3

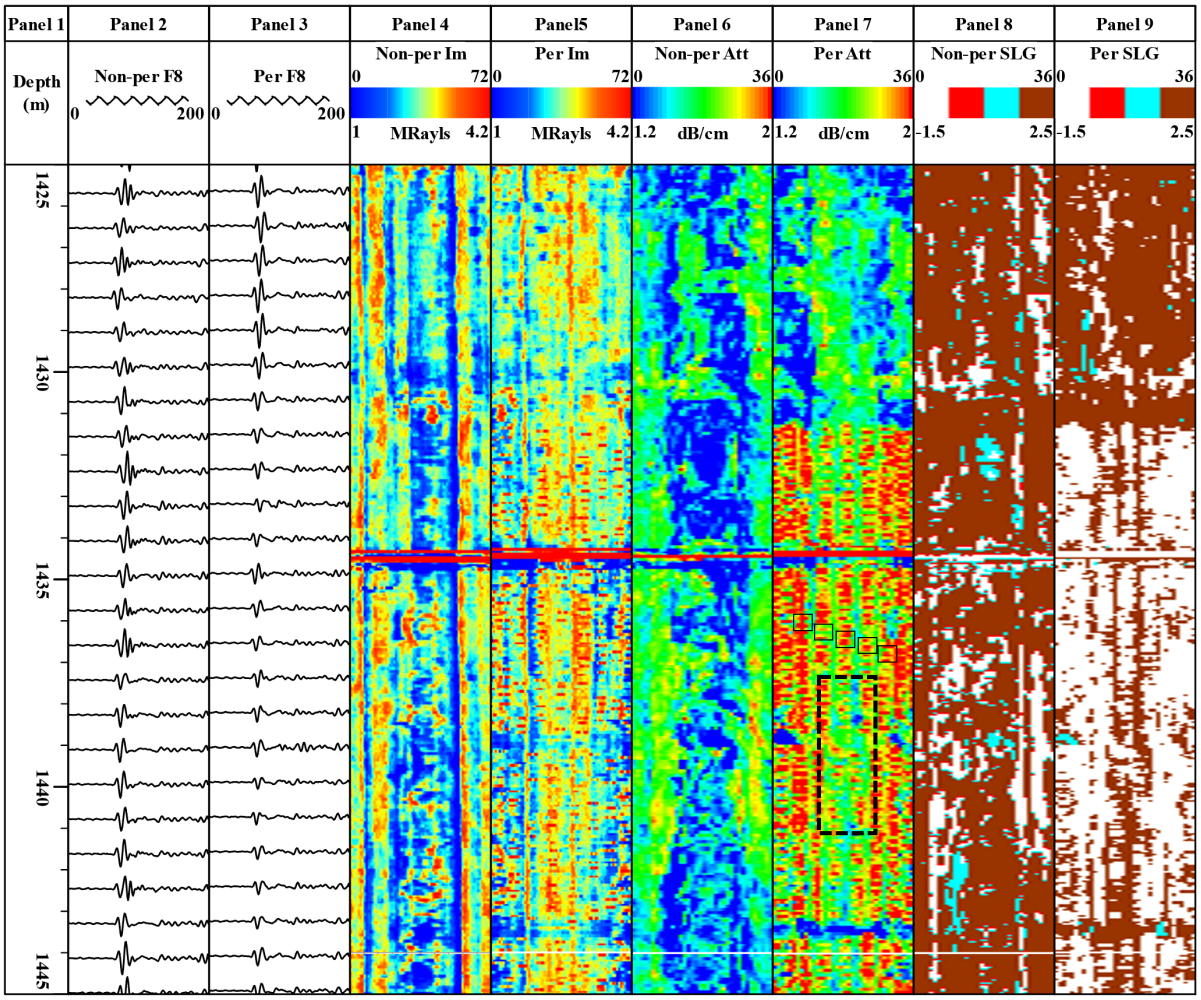

Fig. 5: Results of ultrasonic pitch-catch logging data processing before and after perforation in X casing well.

[5] S. Thierry et al. "Ultrasonic cement logging: Expanding the operating envelope and efficiency". In: *SPWLA Annual Logging Symposium*. SPWLA. 2017, D053S016R006.

[6] D. N. Alleyne and P. Cawley. "The interaction of Lamb waves with defects". In: *IEEE transactions on ultrasonics, ferroelectrics, and frequency control* 39.3 (1992), pp. 381–397.